

# Energized oxygen in the magnetotail : Current Sheet Bifurcation from Speiser motion

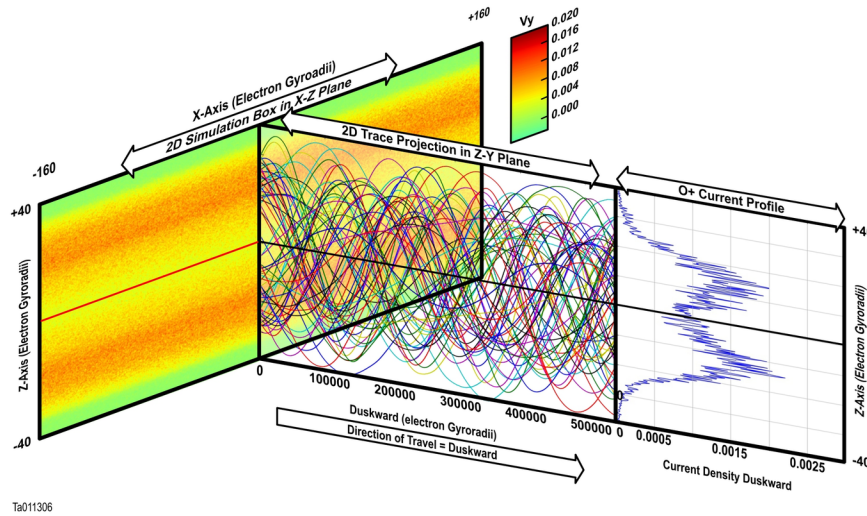
Don George<sup>1</sup> and Jorg-Micha Jahn<sup>1</sup>

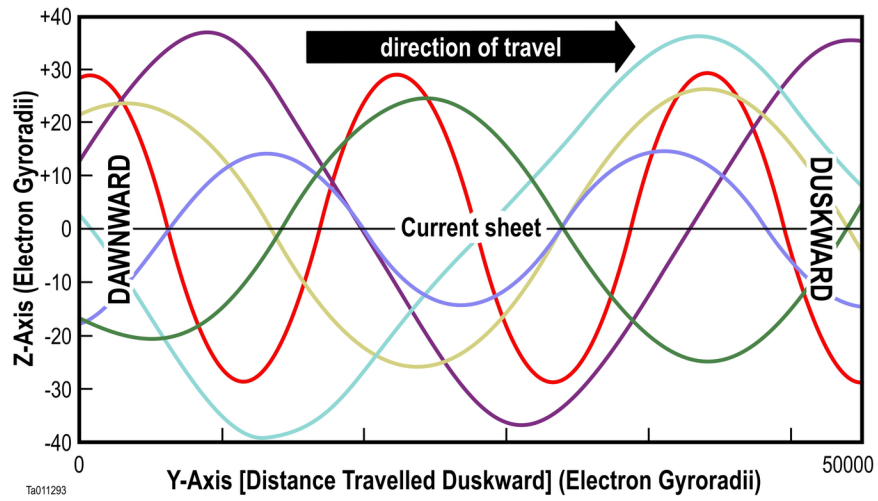
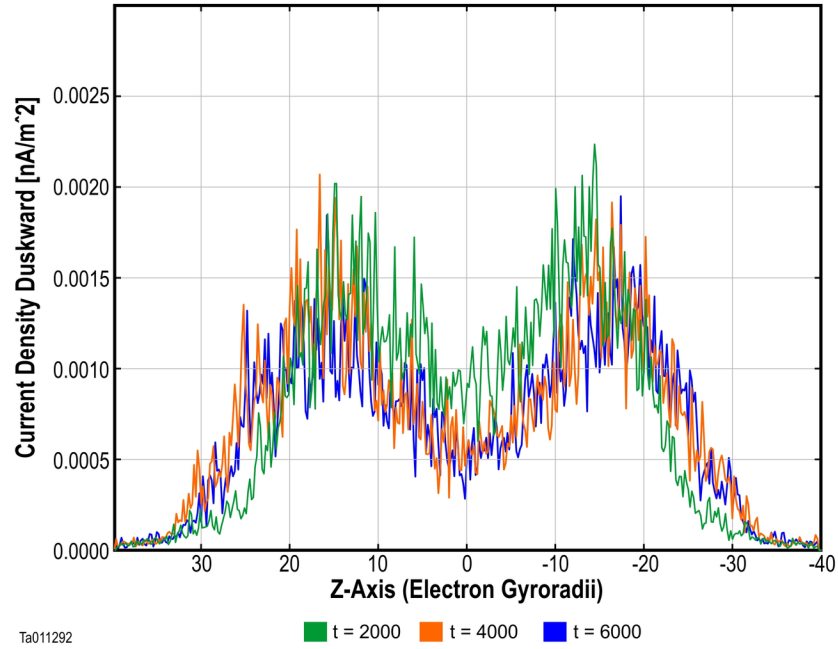
<sup>1</sup>Southwest Research Institute

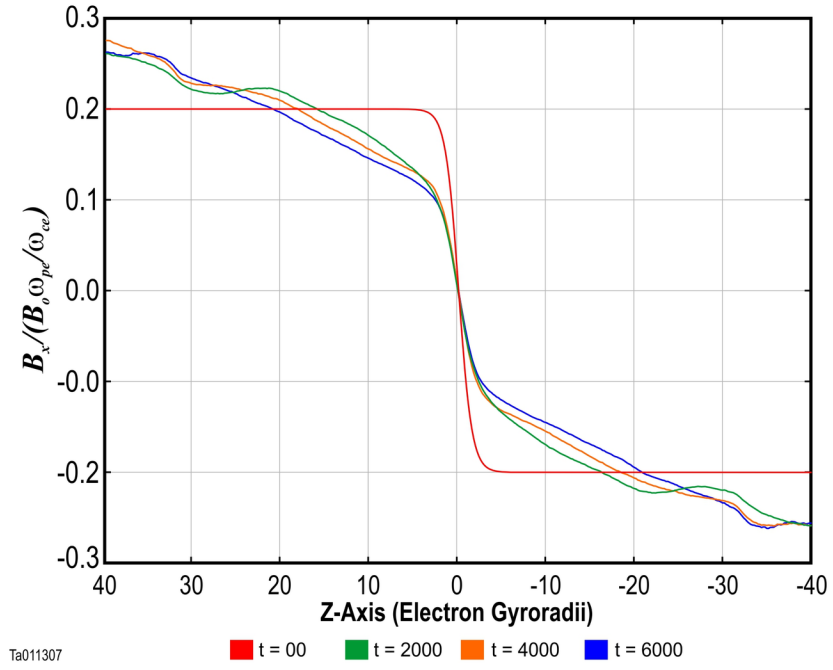
November 21, 2022

## Abstract

Oxygen ions can be a major constituent of magnetospheric plasma, yet the role of oxygen in the magnetosphere is often not sufficiently understood. We examine the case of a thinning current sheet prior to the onset of magnetic reconnection. We perform 2.5D PIC simulations of a 3-species system of electrons, protons and heavy ions ( $O^+$ ). We initiated the simulations using the well-known GEM Challenge configuration. Our approach differs from previous simulations involving heavy ions in two important aspects. First, we initiate the simulations with energized  $O^+$  as opposed to using a thermal population. The energization is based on published in-situ measurements consisting of an initial dusk-ward velocity equivalent to  $\sim 7$  KeV. Second, we tracked the particles directly in the simulation rather than performing test particle tracing in post processing. We show three main results. First, energized dawn-dusk streaming ions exhibit sustained Speiser motion. Second, a single population of heavy ions can produce a stable bifurcated current sheet. Third, magnetic reconnection is not required to produce a bifurcated current sheet.







Ta011307

# Energized oxygen in the magnetotail : Current Sheet Bifurcation from Speiser motion

Don E George<sup>1,2</sup>, Jörg-Micha Jahn<sup>1,2</sup>

<sup>1</sup>Space Science and Engineering, Southwest Research Institute, San Antonio, Texas, USA.

<sup>2</sup>Department of Physics and Astronomy, University of Texas at San Antonio, San Antonio, Texas, USA.

## Key Points:

- Energized dawn-dusk streaming ions exhibit sustained Speiser motion.
- A single population of heavy ions can produce a stable bifurcated current sheet.
- Magnetic reconnection is not required to produce a bifurcated current sheet.

**Abstract**

Oxygen ions can be a major constituent of magnetospheric plasma, yet the role of oxygen in the magnetosphere is often not sufficiently understood. We examine the case of a thinning current sheet prior to the onset of magnetic reconnection. We perform 2.5D PIC simulations of a 3-species system of electrons, protons and heavy ions ( $O^+$ ). We initiated the simulations using the well-known GEM Challenge configuration. Our approach differs from previous simulations involving heavy ions in two important aspects. First, we initiate the simulations with energized  $O^+$  as opposed to using a thermal population. The energization is based on published in-situ measurements consisting of an initial duskward velocity equivalent to  $\sim 7$  KeV. Second, we tracked the particles directly in the simulation rather than performing test particle tracing in post processing.

We show three main results. First, energized dawn-dusk streaming ions exhibit sustained Speiser motion. Second, a single population of heavy ions can produce a stable bifurcated current sheet. Third, magnetic reconnection is not required to produce a bifurcated current sheet.

**1 Introduction****1.1 Background**

The behavior of individual charged particles in magnetic and electric fields is well understood. The behavior of populations of charged particles in a complex and time variable magnetized plasma environment, such as the case of the Earth's magnetotail, is not well understood.

Singly charged oxygen ions were first measured in the magnetosphere by Shelley et al. (1972). The presence of  $O^+$  in these populations affects basic current sheet behavior and the complex behavior of magnetic reconnection and sub-storm dynamics. The complexities of magnetized plasmas with significant amounts of heavy ions involved in current sheet formation and magnetic reconnection is not well understood. There are many hypotheses explaining the role of  $O^+$  and other heavy ions in thin current sheets. For a full review see Kronberg et al. (2014).

A central concept to magnetic reconnection is the current sheet (CS) that forms at the boundary between two regions in space. In general current sheet thicknesses can vary considerably (half thickness of 650 km to 4700 km) (V. A. Sergeev et al., 1993; Runov

et al., 2006). A CS, in its most basic form, has a centrally peaked current distribution and is referred to as a Harris current sheet (Harris, 1962). Observations show that actual current sheets often have a more complex spatial distribution. A double-peaked or bifurcated current sheet (BCS) differs markedly from the Harris-type current sheet (Thompson et al., 2006). The BCS name is not universally accepted, other names include double-humped, split, double, transient-orbits, or as having two off-center current peaks. Bifurcation is often explained as an actual division of the central current sheet into two separate regions. (Wygant et al., 2005; Israelevich & Ershkovich, 2006; Zelenyĭ et al., 2003; Thompson et al., 2006; Sitnov et al., 2006). In this paper we refer to a BCS only as it is found from dawn to dusk across the magnetotail. We do not refer to island formation or outflow bifurcation as used in magnetic reconnection.

Individual charged particles may become trapped in the magnetic null of a CS. Trapped particles gyro-rotate back and forth across the CS. Once trapped they will be accelerated along the CS by the cross-tail electric field. This guiding-center behavior is best described by the term Speiser Orbits or, when there is little or no duskward velocity component, as "cucumber orbits" (Zelenyĭ et al., 2003). Terms like meandering, non-gyrotropic, non-adiabatic and serpentine are also often used to generically describe this motion. We use the term Speiser motion or Speiser orbits (Speiser, 1965) to describe the motion of individual particles involving repeated crossings of the magnetic null of the CS.

Dalena et al. (2010) show that thermal  $O^+$  and  $H^+$  test particles can become trapped in the current sheet of the magnetotail and assume Speiser orbits. They used test particle simulations to predict that, for a statistical ensemble of concurrent nonadiabatic ion trajectories (i.e. in Speiser orbits), a bifurcated current sheet would be produced. In this paper we demonstrate that this prediction is correct.

## 1.2 BCS Observations

BCS observations in the magnetotail current sheet are common with half-thickness ranging from 60 km to 4000 km (Cai et al., 2008; Kistler et al., 2005; Dalena et al., 2010; Hoshino et al., 1996; Runov, Nakamura, Baumjohann, Zhang, et al., 2003; Runov et al., 2004; Nakamura et al., 2002; Wygant et al., 2005; Asano et al., 2004). The key indicator of a BCS is the double-humped current distribution centered around the magnetic null of a current sheet. It is considered a deviation from the single peaked Harris model.

72 The majority of observations of a BCS have scale sizes of hundreds of kilometers, with  
 73 the overall occurrence of bifurcated sheets among stable (non-flapping) thin (about four  
 74 ion gyroradii) current sheets being 17% Asano et al. (2005). This corresponds to a scale  
 75 of a few  $H^+$  gyro-radii. A significant number of BCS encounters show thicknesses of thou-  
 76 sands of kilometers. As this half-thickness is not consistent with proton-only CS they  
 77 are often assumed to be due to heavier ions such as  $O^+$ . Recent observations have defini-  
 78 tively linked the presence of  $O^+$  to these larger scale bifurcations (Runov et al., 2006).

### 79 1.3 BCS Causes

80 There are several mechanisms for the formation of the double-peaked current sheets  
 81 (Asano et al., 2004). Presently there are two main categories of possible causes for cur-  
 82 rent sheet bifurcation. First, a wide variety of bulk plasma properties, anisotropies and  
 83 instabilities are attributed to the production of a BCS:

- 84 • Cowley (1978) predicted the existence of a bifurcated current sheet due to a pres-  
 85 sure anisotropy where  $P_{\perp} > P_{\parallel}$ . Here a broad region of depressed fields devel-  
 86 ops at the center of the current sheet. This central region terminates at its outer  
 87 boundary by a spike in the current density. These spikes on either side of the cen-  
 88 tral region form the bifurcation.
- 89 • Sitnov et al. (2003) associated bifurcation with a small ion temperature anisotropy  
 90 for pancake distributions where  $T_{\perp} > T_{\parallel}$ .
- 91 • Splitting of the current sheet (i.e bifurcation) can be due to the nonadiabatic scat-  
 92 tering of particles in a strongly curved magnetic field of a thin current sheet (Zelený  
 93 et al., 2003).
- 94 • A 'bifurcated' current sheet can be explained in terms of a traveling (ion-ion) kink  
 95 displacement with a single continuous displacement into both hemispheres (Karimabadi  
 96 et al., 2003).
- 97 • Bifurcation of the current density distribution may not depend on an anisotropy  
 98 of the  $T_{ion\parallel} > T_{ion\perp}$ , but rather on the anisotropy of the  $T_{\perp}$  alone (Israelevich  
 99 & Ershkovich, 2008) .
- 100 • The source of observed bifurcation to be a result of either a sausage mode or a kink  
 101 mode propagating dawn to dusk (Runov, Nakamura, Baumjohann, Zhang, et al.,  
 102 2003).

- 103 • Bifurcation can be due to the non-diagonal terms of the pressure tensor and tem-  
104 perature anisotropy (Holland & Chen, 1993).
- 105 • Not only bifurcation but also current sheet flapping and reconnection can all be  
106 explained as a consequence of various instabilities (Kelvin-Helmholtz, LDHI, and  
107 tearing), affecting a Harris current sheet (Ricci et al., 2004).
- 108 • Nonlinear development strongly modifies the electron flow velocity in the central  
109 region, which induces a bifurcation of the current density (Daughton et al., 2004).
- 110 • The main contribution to the current comes from ions, but the bifurcated shape  
111 is supported by electrons due to the pressure gradient of their distribution and elec-  
112 tric drift terms (Greco et al., 2007).

113 The second category of causes for bifurcation is magnetic reconnection. Many ob-  
114 servations conclude that current sheet bifurcation is a direct product of reconnection (Hoshino  
115 et al., 1996; Eastwood et al., 2008; Lottermoser et al., 1998; Karimabadi et al., 2005).  
116 There are many instances of bifurcation associated with reconnection outflow (earthward  
117 and tailward)(e.g. (Runov, Nakamura, Baumjohann, Treumann, et al., 2003).

118 However, many observations lead to the conclusion that current sheet bifurcation  
119 is independent of magnetic reconnection (Dalena et al., 2010; Runov et al., 2004; Ricci  
120 et al., 2004; Runov, Nakamura, Baumjohann, Zhang, et al., 2003; Daughton et al., 2004).  
121 Thompson et al. (2006), who argued for association with magnetic reconnection, also in-  
122 dicated that a statistical analysis of identified BCSs show that they can exist well away  
123 from the region of magnetic reconnection.

124 Overall it remains an open question what process leads to the formation of a bi-  
125 furcated current sheet.

#### 126 **1.4 Oxygen Energization**

127 The dawn-dusk electric field across the magnetotail CS predicts cross-tail ion ac-  
128 celeration as evidenced by a increased dusk-side asymmetry of energized ions (Speiser,  
129 1965; Lyons & Speiser, 1982; Meng et al., 1981). Several investigations of cross-tail elec-  
130 tric field acceleration of protons and  $O^+$  have been undertaken resulting in acceleration  
131 estimates of  $>50$  keV  $O^+$  (Birn et al., 2001) , 100-200 keV  $H^+$  (Birn et al., 2004)), 20

132 keV  $O^+$  (Ipavich et al., 1984)), 50-500 keV  $H^+$  (Meng et al., 1981), and 112-157 keV  $O^+$   
 133 (Wygant et al., 2005). Without regard to the mechanism, accelerated  $O^+$  in the 12 to  
 134 40 keV range has been observed by (Kistler et al., 2005) streaming dawn-dusk in the mag-  
 135 netotail at about 19 RE. Even for a typical quiet-time cross-tail field of 0.5 V/m a ther-  
 136 mal  $O^+$  atom could easily gain up to  $12keV$  from the cross-tail potential alone stream-  
 137 ing only a quarter to halfway across the magnetotail (Baker & Pulkkinen, 1998). See Kronberg  
 138 et al. (2014) for an overall review of the transport and acceleration of heavy ions in the  
 139 magnetosphere and tail.

## 140 **2 Simulations**

141 No previous work has performed kinetic plasma simulations which included ener-  
 142 gized  $O^+$ . We performed 3-species 2.5D PIC simulations (explained below) of a thin cur-  
 143 rent sheet. Our simulations build upon similar simulations limited to thermal  $O^+$  (Markidis  
 144 et al., 2011; Karimabadi et al., 2011) and also on work using energized  $O^+$  test parti-  
 145 cles in a magnetic field model (Dalena et al., 2010). We begin with an investigation of  
 146 the individual and group kinetic behaviors of energized  $O^+$  followed by an analysis of  
 147 bulk current sheet properties. Our simulation culminates in the generation of a sustain-  
 148 able bifurcated current sheet.

### 149 **2.1 Simulation Methodology**

150 Our simulations begin with a 3-species plasma consisting of electrons, protons and  
 151 oxygen ions. We base this on the well-known GEM Challenge configuration (Birn et al.,  
 152 2004). This 2-species configuration served as a baseline for comparisons to previous sim-  
 153 ulation methods. We modified the plasma by including a thermal oxygen background,  
 154 adding a small duskward velocity component assuming that energization stems from the  
 155 cross-tail electric field. This is, of course, not the only source of energization in the mag-  
 156 netotail. The energization of the  $O^+$  has not previously been investigated via kinetic PIC  
 157 simulations.

### 158 **2.2 PIC Code**

159 Simulations involving thin current sheets and magnetic reconnection use PIC codes  
 160 extensively (Hesse et al., 2001; Hesse & Birn, 2004; Hesse et al., 1999; Hesse & Schindler,

161 2001; Karimabadi et al., 2011; Shay et al., 2007). This investigation uses a 2.5D, fully  
 162 electromagnetic, Particle-In-Cell (PIC) code (Hesse & Schindler, 2001). The code is struc-  
 163 tured on a rectangular grid of cells of the Buneman type (Villasenor & Buneman, 1992).  
 164 Charged particles have a rectangular charge function. They are distributed throughout  
 165 a rectangular two dimensional grid. Electric and magnetic fields reside in the center of  
 166 each cell. In a 2.5D simulation the particle positions are calculated in 2D while the par-  
 167 ticle velocities, electric fields and magnetic fields are calculated in 3D. Hence the des-  
 168 ignation of 2.5D.

169 Particles are tracked at sub-grid positions while fields are tracked only at the cen-  
 170 ter of each cell. Bulk simulation properties are also calculated at the center of each cell.  
 171 Particles and fields are advanced in an alternating fashion via a staggered leapfrog method.  
 172 Particle positions and particle velocity changes are advanced out of phase by one-half  
 173 time step. Similarly, magnetic field and currents are advanced out of phase with the elec-  
 174 tric fields by one-half time step. New particle parameters are calculated from the pre-  
 175 vious fields by solving the equations of motion. Previous time-step fields are interpolated  
 176 to the particle sub-grid positions. New field parameters are calculated from particle charge  
 177 and current densities by solving Maxwells equations. The resulting densities are gath-  
 178 ered on the grid vertices. For a detailed explanation see Birdsall and Langdon (1991)).

179 The time-step is chosen to ensure convergence of the field equations and to meet  
 180 the Courant-Friedrichs-Lewy (CFL) condition of  $C_r = V_{max} \frac{\Delta T}{\Delta X} \leq 1$ . Implicit time in-  
 181 tegration of the fields dampens oscillatory behavior of electromagnetic waves. To ensure  
 182 charge conservation an iterative "Langdon-Marder" type correction is applied to the elec-  
 183 tric field values (Bruce Langdon, 1992).

184 All simulations were performed on a DELL PowerEdge 2900 system with a 3 GHz  
 185 Quad-Core Intel Xenon 5300 Processor, 48 Gbytes of RAM and 8 TBytes of local hard  
 186 drive storage. No parallelization was employed. We performed 800 x 400 grid simula-  
 187 tions with  $10^8$  macro-particles run at a typical rate of 200 time-steps (i.e. electron gyro-  
 188 periods) per computational hour. This resulted in a 6000 time-step computation time  
 189 of 30 hours.

## 190 2.3 Simulation Setup

191 The simulation region is oriented such that it corresponds to the GSM X-Z plane  
 192 in the center of Earth’s magnetosphere at  $Y=0$ . Y corresponds to the GSM out-of-plane  
 193 direction. Due to the finite size of the simulation box, boundary conditions have been  
 194 set along all three axis, in keeping with previous PIC simulations. For particles, the X  
 195 boundaries are periodic. Any particle exiting one side reenters the opposite side with the  
 196 same velocity vector. The Z boundaries are specularly reflecting. Any particle exiting  
 197 the  $\pm Z$  boundary will reenter at the same location but with the opposite  $V_z$ .

198 Y position is calculated for particles during post-processing. They do not “move”  
 199 in Y during the simulation. There is, however, an implicit assumption that the bound-  
 200 aries in Y are periodic. This means that for each particle that “exits” along Y another  
 201 identical particle “reenters” from the opposite side with the same 3D velocity. From the  
 202 viewpoint of the simulation the particle has not moved.

203 For the electric and magnetic fields the X boundaries are periodic and continuous.  
 204 Electric and magnetic fields are zero outside the simulation box. The Z boundaries are  
 205 simple reflecting boundaries such that an exiting particle will reenter at the same point  
 206 with the same  $V_x$  and  $V_y$  but opposite  $V_z$ . This is accounted for in the implicit integra-  
 207 tion performed in the field calculations. Scaling and normalization of simulation param-  
 208 eters is unitless.

209 While the 2D box has no Y dimension per se, we track  $V_y$  to integrate the Y dis-  
 210 placement for each particle during post-processing. The ratio between the electron plasma  
 211 and gyro frequencies is 5. This establishes the relationship between  $B_o$  and  $n_o$ .  $B_o$  is the  
 212 peak magnetic field strength in the surrounding bulk plasma.  $n_o$  is the initial peak den-  
 213 sity at the center of the current sheet.

## 214 2.4 Initial Conditions

### 215 2.4.1 Basic Configuration

216 Our simulation setup uses the GEM reconnection challenge setup with minor vari-  
 217 ations to accommodate the larger oxygen gyro-radius. The simulation box is  $320 \times 160$   
 218 electron gyro-radii compared to the GEM challenge which used a  $128 \times 64$  box while the  
 219 computational grid is  $800 \times 400$  nodes. The initial magnetic field configuration repre-

220 sents an anti-parallel magnetotail. We follow the same  $B_x(z)$  magnetic field profile as  
 221 used in the GEM Challenge. Since our goal was not to "speed up" the simulation we var-  
 222 ied from the GEM Challenge by not including a magnetic island perturbation. The GEM  
 223 Challenge employed a CS half-thickness of 0.5 ( $\lambda=0.5$ ) ion (proton) gyro-radii. We ini-  
 224 tialized the CS half thickness to a value of 1.5 ion (proton) gyro-radii. This variation fur-  
 225 ther avoided the onset of magnetic reconnection. This allowed us more time to study the  
 226 evolution of the CS.

### 227 **2.4.2 Mass Ratios**

228 In an ideal simulation the relative masses of the species would reflect physical ra-  
 229 tios. This is both computationally prohibitive and unnecessary. Our study uses  $m_e/m_{H^+}/m_{O^+}$  mass  
 230 ratios of 1/25/250. Previous kinetic studies have shown that these mass ratios, while not  
 231 physical, are more than sufficient to study oxygen dynamics.

232 Kinetic simulations using the GEM challenge with  $m_p/m_e$  mass ratios of 25, 180  
 233 and 1836 mass ratios had no effect on the larger-scale phenomena (Ricci et al., 2002);  
 234 the evolution of 2-species reconnection was nearly identical for  $m_i/m_e$  of 9, 25, 64, and  
 235 100 (Hesse et al., 1999); a ratio of 25 separates the relevant electron physics from the  
 236 proton physics. We assume that the chosen mass ratios, are sufficient for the study of  
 237 magnetic reconnection and are also sufficient for the study of the CS prior to reconnec-  
 238 tion onset.

239 When comparing mass ratios, Markidis et al. (2011) who used physical masses and  
 240 Karimabadi et al. (2011) who used reduced mass ratios of 1/10/90, reported separation  
 241 of scale between the three species for studies of both pre- and post-reconnection evolu-  
 242 tion. For our study we use  $m_e/m_{H^+}/m_{O^+}$  mass ratios of 1/25/250, which are therefor  
 243 more than sufficient to separate the mass effects of the species. Even smaller mass ra-  
 244 tios could have been employed to evaluate the kinetic effects studied here, however, we  
 245 opted for higher ratios in preparation for future studies involving the effect of  $O^+$  on mag-  
 246 netic reconnection.

### 247 **2.4.3 $O^+$ Energization**

248 Our  $O^+$  initial conditions are distinctly different from those performed in previ-  
 249 ous simulation studies which used backgrounds of  $O^+$  in the thermal range (Markidis

250 et al., 2011; Hesse & Birn, 2004; Karimabadi et al., 2011). What is new in this work is  
 251 that we "energize" the  $O^+$ . This energization is achieved by giving the thermal back-  
 252 ground a duskward  $V_y$  velocity. The initial thermal background of  $O^+$  is energized by  
 253 the addition of a  $V_y$  component. We add this uniform initial velocity in the duskward  
 254 direction. We found that an initial  $V_y$  equivalent to  $\sim 25$  keV would stabilize to  $\sim 7$  keV  
 255 after only a few time-steps. We accept that this impulsive initial push is non-physical,  
 256 however, it quickly relaxes to a value observed in the magnetotail.

### 257 2.5 Test Particles

258 The PIC simulation is a numerical kinetic treatment of plasma particles. The ad-  
 259 ditional introduction of specific test particles is not needed. The simulation code calcu-  
 260 lates 2D positions and 3D velocities of 100 million particles. Strictly speaking they are  
 261 actually macro-particles, yet they behave as individual particles would. Due to the 2D  
 262 nature of the simulation the Y position is not tracked for particles. We calculate a Y dis-  
 263 placement from the  $V_y$  at each time-step during post-processing. This Y displacement  
 264 is in electron gyro-radii as are the X and Z dimensions. The assumption of periodic bound-  
 265 ary conditions in the Y direction allows for this. Integration of subsequent Y displace-  
 266 ments in this manner allows us to examine the kinetics of individule particles in 3D over  
 267 time.

### 268 3 Simulation Results

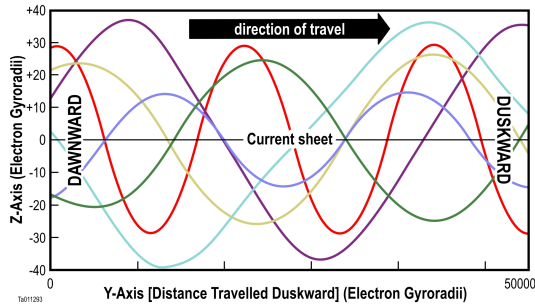


**Figure 1.** Six representative  $O^+$  ion trajectories along the Y-axis (duskward to the right) following Speiser orbits along  $\pm Z$  that cross the current sheet at  $Z=0$ , indicated by the horizontal line across the center.

269

### 3.1 Individual Test Particle Motion

270

271

272

273

274

275

Figure 1 shows the trajectories of representative  $O^+$  particles. The trajectory of each particle follows a simple sinusoidal curve as it gyro-rotates across the CS while simultaneously moving along +Y duskward.. Thousands of particles (macro-particles) show this same type of trajectory. For clarity only 6 trajectories are shown in Figure 1 while Figure 5 shows 100 representative  $O^+$  particles. These sinusoidal tracks indicating Speiser motion as a result of the applied energization.

276

All  $O^+$  particles accelerated in the simulation exhibit sustained Speiser motion.

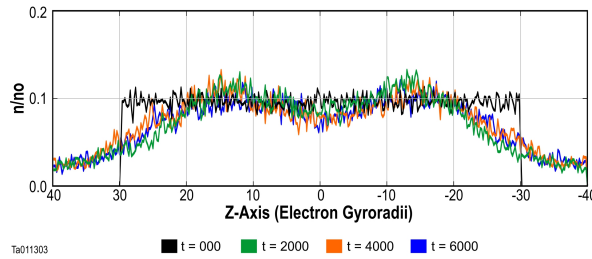


**Figure 2.** Cross section of  $[O^+]$  (density) along Z at X=0 ( $e^-$  gyro-radii) for four time-steps (0, 2000, 4000, 6000  $e^-$  gyro-periods). This clearly shows that even though the  $O^+$  ions are moving throughout the Z range, the  $O^+$  density profile ( $n/n_o$ ) remains constant over time.

277

### 3.2 Density Distribution

278

279

280

281

282

We initiated our simulation with a homogeneous density for all three species.  $H^+$  was set to  $0.1 n_o$  over the entire simulation box.  $O^+$  was also set to  $0.1 n_o$  over all X locations but only over the Z range of  $\pm 30$  electron gyro-radii. This reduced the heavy ion interaction with the Z boundaries. The  $e^-$  distribution was matched to that of the ions to maintain quasi-neutrality of the plasma.

283

284

285

286

287

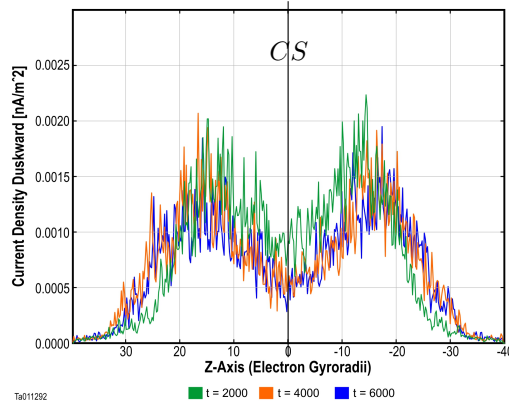
288

Figure 2 shows the density distribution of  $O^+$  at  $t=0$  and three later timesteps. The distribution remains flat over time, consistent with observations (V. Sergeev et al., 2003) and the evolution of BCS models (Sitnov et al., 2003). More importantly this clearly shows that there is no actual separation of the population into two parts. It is not the particle distribution that is producing the bifurcation. Figure 1 shows the  $O^+$  population moving back and forth across the current sheet. This motion indicates that the gyro-centers

289 of this population remain on the neutral line. Therefore, the source of bifurcation must  
 290 have a different cause than the population splitting.

### 291 3.3 Current Distribution

292 The primary indication of a BCS is the double-humped current distribution found  
 293 along the current sheet. Figure 3 shows a cross section of the  $O^+$  contribution to  $J_y$  cut  
 294 along  $Z$  at the center ( $X=0$ ). First, as it was initialized and then at three later time-steps.  
 295 This indicates the presence of a BCS with the distinctive double peak with a much lower  
 296 current in the center. We can attribute the two peaks to a single population of  $O^+$  un-  
 297 dergoing gyrorotation along Speiser orbits. This is due to the particle velocity distribu-  
 298 tion being primarily along the  $+Y$  (duskward) axis in the vicinity of both of the current  
 299 peaks.



**Figure 3.** Current flowing in the Y (duskward) direction is calculated by  $O^+$  charge and velocity along the Z axis and integrated over the X axis. A bifurcation in the current centered around the current sheet ( $Z=0 e^-$  gyroradii) is clearly evident by the 'double-humped' shape of the current profile. By overlaying the  $O^+$  current density at three timesteps (2000, 4000, 6000  $e^-$  gyroperiods) in the simulation it is evident that the apparent bifurcation is stable and consistent over time.

### 300 3.4 Magnetic Field

301 Figure 4 shows the Z profile of  $B_x$  at several timesteps during the simulation, start-  
 302 ing from the initial configuration from the GEM challenge Harris Current Sheet.

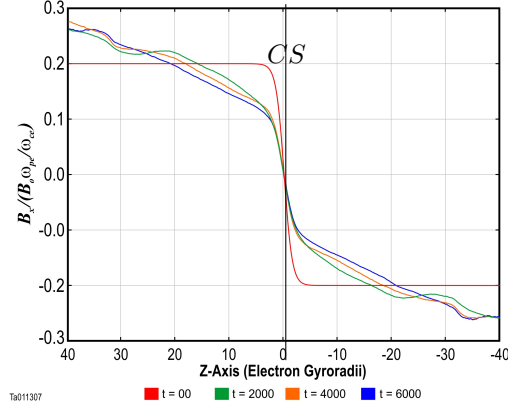


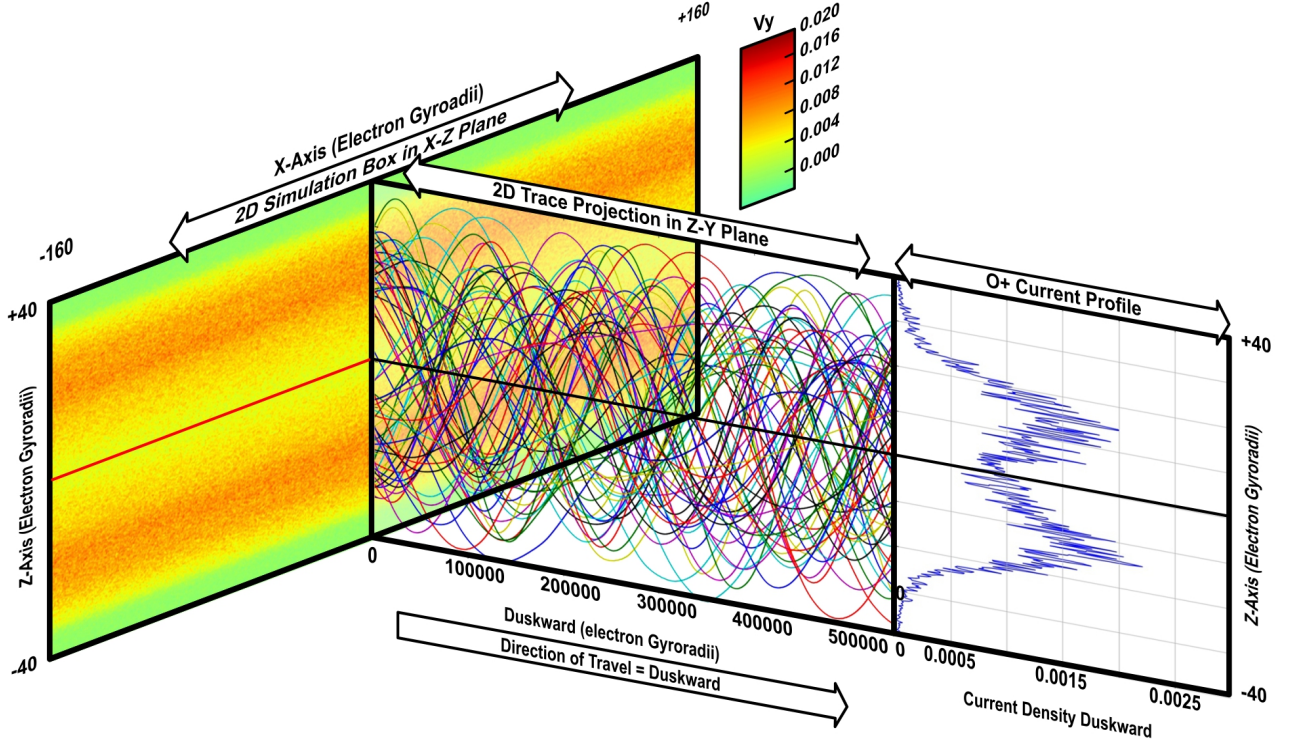
**Figure 4.** Z Profiles of  $B_x$  (for  $x=400 e^-$  gyroradii) at: time = 0 (red); at timestep 2000 ( $e^-$  gyroperiods) with  $O^+$  present (green); at timestep 4000 ( $e^-$  gyroperiods) with  $O^+$  present (orange); timestep 6000 ( $e^-$  gyroperiods) with  $O^+$  present (blue).

303 As time progresses, the Z-profile of  $B_x$  changes. There is some initial flattening  
 304 of the profile although the basic magnetic configuration remains consistent throughout  
 305 the simulation. Likewise, throughout the simulation, the magnetic field configuration re-  
 306 mains that of a Harris current sheet, even with the presence of a bifurcation.

### 307 3.5 Overall System Analysis

308 While Figures 1 and 3 provide important views of the individual particle behav-  
 309 iors of  $O^+$  plasma, Figure 5 provides a view of their relationship to one another. We show  
 310 a composite view of the current sheet in 3D. This shows how particle motion and cur-  
 311 rent distribution relate to one another. This composite view reveals the true nature of  
 312 the bifurcation. We see a bifurcation in the current sheet that is caused by a single "non-  
 313 bifurcated" population of particles. This bifurcation is not a result of the current sheet  
 314 splitting, i.e. due to the particle distribution, rather it is a kinetic effect due to a large  
 315 statistical population all with duskward velocity vectors at the edges of their motion.

316 The 100 sample trajectories in Figure 5 give a visual representation of the large pop-  
 317 ulation moving duskward. Over the entire simulation box there are 100 million  $O^+$  macro-  
 318 particles. This models a physical population found in the magnetotail. Our sample here  
 319 depicts a slice at the center ( $X=0$ ) but is representative across the entire width of the  
 320 box in X.



Ta011306

**Figure 5.** Composite graphic of 1)  $O^+$  velocity in the X-Z plane, 2) 60 trajectory traces of  $O^+$  ions in the Z-Y plane, and 3) the  $O^+$  current profile in Z at X=0 ( $e^-$  gyroradii : center) of the simulation box. Taken at timestep 4000 ( $e^-$  gyroperiods.)

321 Each of these many Speiser orbiting trajectories shown is independent of the oth-  
 322 ers. At the same time all these ions are streaming from dawn to dusk (+Y) and gyro-  
 323 rotate in the +/-Z plane. Plotting 100 or even more particles bears no real sign of the  
 324 bifurcated nature of the current sheet. Only when considering the whole ensemble and  
 325 adding their velocities to get the current profile the bifurcation is revealed.

326 Finally we note that the system had not evolved to the point of onset of magnetic  
 327 reconnection at the end of this simulation. We can conclude that magnetic reconnection  
 328 is not required for the formation of a BCS.

#### 329 4 Discussion

330 In this paper we show three main results. First, energized  $O^+$  accelerated duskward  
 331 exhibits sustained Speiser motion along the current sheet. Second, a single population

332 of heavy ions can produce a stable bifurcated current sheet. Third, magnetic recon-  
 333 nection is not required to produce a bifurcated current sheet.

334 In our simulations bifurcation of a current sheet is purely a result of the kinetic be-  
 335 havior of individual particles. These particles form a single population as opposed to two  
 336 spatially separate populations. The key to bifurcation is the statistical behavior of a large  
 337 single population taken as a whole causing a bifurcated current density. The following  
 338 sequence describes the mechanism. Thermal  $O^+$  ions **of ionospheric origin** migrate  
 339 into the region near the current sheet. Some ions become trapped around the current  
 340 sheet magnetic null. Once trapped the cross-tail potential accelerates them from pure  
 341 gyro-motion to duskward streaming Speiser orbits. As the ions become increasingly en-  
 342 ergized they continue to gyro-rotate in the magnetic field surrounding the null. The op-  
 343 posing directions of the magnetic field lines combines with the duskward acceleration.  
 344 This naturally moves the ions towards the null no matter which side they are on. They  
 345 follow natural kinetic paths referred to as a Speiser orbits. A single, statistically signif-  
 346 icant, population of Speiser orbiting ions then forms the impression of a bifurcated cur-  
 347 rent sheet by virtue of the ensemble average of Speiser orbits.

348 On average, for every ion that is crossing the null in one direction there is one cross-  
 349 ing in the other direction producing a net particle flux of zero across the CS. Since the  
 350 net flux of particles crossing the CS is zero, the net current across the magnetic null is  
 351 also zero.

352 However this leaves only the parallel velocity components, whose velocities on av-  
 353 erage all point in the same direction to produce the current distribution. As each ion moves  
 354 away from the null into the bulk magnetic field,  $V \times B$  forces turn it back towards the null.  
 355 This occurs at a distance from the null on the order of the ion gyro-radius. At their fur-  
 356 thest distance from the CS (+/-Z) their velocity vector is duskward and parallel to the  
 357 CS.

358 The velocity vectors multiplied by the ion charge yields a current. Adding Y ve-  
 359 locity components across the CS forms the simulation current profile that peaks on ei-  
 360 ther side of the CS. The particle velocities of ions crossing the CS null are primarily in  
 361 the Z direction. Thus, rendering the current near the null, the current profile is reduced.  
 362 Taken together this produces a double-humped current profile which is the very defini-

363 tion of a bifurcated current sheet. All this occurs without ever splitting the  $O^+$  popu-  
 364 lation into separate populations.

365 Zelenyĭ et al. (2003) states that Speiser orbits form the basic current of the sheet.  
 366 Yet, they attribute the bifurcated structure to quasi-adiabatic ‘cucumber’ orbits. Our  
 367 work demonstrates that Speiser orbits do produce a bifurcation in the current sheet. In-  
 368 stead, quasi-adiabatic (a.k.a. cucumber or quasi-trapped) orbits (Buchner & Zelenyi, 1989)  
 369 should be considered a degenerate energy case of Speiser orbits. This means that a cu-  
 370 cumber orbit should be a Speiser orbit with a zero or near-zero velocity component along  
 371 the current sheet. In addition to the PIC simulations performed for this work, we per-  
 372 formed simulations of particles in a static 2D CS. These results show that it is common  
 373 for a trapped particle to assume a cucumber orbit. It also shows that a particle in a cu-  
 374 cumber orbit need only be accelerated a tiny fraction of its energy to ”assume” a more  
 375 general Speiser orbit. Such acceleration is easily obtained by the cross-tail electric field.

376 Comparing a statistical number cucumber orbiting particles to Speiser orbiting par-  
 377 ticles shows that they could both produce a bifurcated current sheet. This is apparent  
 378 since both have the same zero net-flux across the CS and both have duskward velocity  
 379 vectors as they gyro-rotate back towards the CS. A sustained cucumber orbit would be  
 380 difficult to achieve since even a small acceleration turns it into a Speiser orbit. A sus-  
 381 tained statistical population of cucumber orbits would not exist in a physical current sheet  
 382 due to the presence of the dawn-dusk E-field.

383 We conclude that it is incorrect to refer to a BCS as two separate currents of a sin-  
 384 gular particle population or as two separate populations. A BCS can be viewed as a purely  
 385 kinetic phenomenon. It is the result of the superposition of all particles in a Speiser or-  
 386 biting population onto an underlying Harris type current sheet. This is not to say that  
 387 there are no secondary effects by other species, CS structure or magnetic reconnection.  
 388 However these will be explored further in future work. We can argue that lower energy  
 389 particles gyro-rotate closer to the CS and higher energy particles further away. This pro-  
 390 duces a bifurcation whose current profile mimics that of the energy distribution. It is  
 391 obvious that the depth of penetration into the bulk regions outside the CS follow the en-  
 392 ergy distribution of the ions.

## 5 Summary

Our work investigated the kinetic behavior of a bifurcated current sheet. We performed 2.5D kinetic PIC simulations of a 3-species plasma consisting of electrons, protons and heavy ions ( $O^+$ ). A magnetotail-like Harris current sheet configuration was used in following with the GEM Challenge model. To the GEM challenge population of electrons and protons we superimposed a population of thermal  $O^+$  ions. We energized this homogeneous  $O^+$  population with a dusk-ward velocity, equivalent to  $\sim 7$ keV. Individual  $O^+$  particles involved directly in the simulation were tracked throughout the simulations. Post-processing extrapolated the 2D positions and out-of-plane velocities of particles to examine their kinetic behavior in 3D.

Three primary conclusions have been drawn by this investigation. Dawn-dusk streaming  $O^+$  exhibits sustained Speiser motion. A single, statistical, population of heavy ions produces a stable bifurcated current sheet. There is no splitting or division of the ion population. This stable  $O^+$  bifurcated current sheet can exist independently of any magnetic reconnection process.

Previous works have studied the behavior of thermal heavy ions in a current sheet. Energization of these heavy ions is the key to forming a bifurcated current sheet. It is also the key to understanding the nature of the effect of heavy ions on processes in a current sheet. Future work will examine the effect of the energized  $O^+$  population on magnetic reconnection.

## Acknowledgments

The authors thank Micheal Hesse, formerly of NASA GSFC, for providing the PIC code used in this work and instruction in its use.

The simulation results used in this study are available at the following repository: <https://doi.org/TBD> located in <https://zenodo.org/communities/plasma-pic-simulation/>.

## References

- Asano, Y., Mukai, T., Hoshino, M., Saito, Y., Hayakawa, H., & Nagai, T. (2004, May). Statistical study of thin current sheet evolution around substorm onset. *Journal of Geophysical Research (Space Physics)*, *109*(A5), A05213. doi:

- 423 10.1029/2004JA010413
- 424 Asano, Y., Nakamura, R., Baumjohann, W., Runov, A., Vörös, Z., Volwerk, M.,  
425 ... Rème, H. (2005). How typical are atypical current sheets? *Geophysical*  
426 *Research Letters*, *32*, issue 3.
- 427 Baker, D. N., & Pulkkinen, T. I. (1998). Large-Scale Structure of the Magneto-  
428 sphere. *Washington DC American Geophysical Union Geophysical Monograph*  
429 *Series*, *105*, 21. doi: 10.1029/GM105p0021
- 430 Birdsall, C., & Langdon, A. (1991). *Plasma physics via computer simulation*. Taylor  
431 and Francis.
- 432 Birn, J., Drake, J. F., Shay, M. A., Rogers, B. N., Denton, R. E., Hesse, M., ...  
433 Otto, A. (2001, Mar). Geospace Environmental Modeling (GEM) magnetic  
434 reconnection challenge. *Journal of Geophysical Research (Space Physics)*,  
435 *106*(A3), 3715-3720. doi: 10.1029/1999JA900449
- 436 Birn, J., Thomsen, M., & Hesse, M. (2004, Apr). Acceleration of oxygen ions in the  
437 dynamic magnetotail. *Annales Geophysicae*, *22*(4), 1305-1315. doi: 10.5194/  
438 angeo-22-1305-2004
- 439 Bruce Langdon, A. (1992, July). On enforcing Gauss' law in electromagnetic  
440 particle-in-cell codes. *Computer Physics Communications*, *70*, 447-450. doi:  
441 10.1016/0010-4655(92)90105-8
- 442 Buchner, J., & Zelenyi, L. M. (1989, Sep). Regular and chaotic charged particle  
443 motion in magnetotaillike field reversals. 1. Basic theory of trapped motion.  
444 *Journal of Geophysical Research (Space Physics)*, *94*(A9), 11821-11842. doi:  
445 10.1029/JA094iA09p11821
- 446 Cai, C. L., Dandouras, I., Rème, H., Cao, J. B., Zhou, G. C., & Parks, G. K. (2008,  
447 May). Cluster observations on the thin current sheet in the magnetotail. *An-*  
448 *nales Geophysicae*, *26*(4), 929-940. doi: 10.5194/angeo-26-929-2008
- 449 Cowley, S. W. H. (1978, Nov). The effect of pressure anisotropy on the equilibrium  
450 structure of magnetic current sheets. *Planetary and Space Science*, *26*(11),  
451 1037-1061. doi: 10.1016/0032-0633(78)90028-4
- 452 Dalena, S., Greco, A., Zimbardo, G., & Veltri, P. (2010, Mar). Role of oxy-  
453 gen ions in the formation of a bifurcated current sheet in the magnetotail.  
454 *Journal of Geophysical Research (Space Physics)*, *115*(A3), A03213. doi:  
455 10.1029/2009JA014710

- 456 Daughton, W., Lapenta, G., & Ricci, P. (2004, Sep). Nonlinear Evolution of the  
457 Lower-Hybrid Drift Instability in a Current Sheet. *Physical Review Letters*,  
458 *93*(10), 105004. doi: 10.1103/PhysRevLett.93.105004
- 459 Eastwood, J. P., Brain, D. A., Halekas, J. S., Drake, J. F., Phan, T. D., Øieroset,  
460 M., . . . Acuña, M. (2008, Jan). Evidence for collisionless magnetic re-  
461 connection at Mars. *Geophysical Research Letters*, *35*(2), L02106. doi:  
462 10.1029/2007GL032289
- 463 Greco, A., de Bartolo, R., Zimbardo, G., & Veltri, P. (2007, Jun). A three-  
464 dimensional kinetic-fluid numerical code to study the equilibrium structure  
465 of the magnetotail: The role of electrons in the formation of the bifurcated  
466 current sheet. *Journal of Geophysical Research (Space Physics)*, *112*(A6),  
467 A06218. doi: 10.1029/2007JA012394
- 468 Harris, E. G. (1962, January). On a plasma sheath separating regions of oppo-  
469 sitely directed magnetic field. *Il Nuovo Cimento*, *23*, 115-121. doi: 10.1007/  
470 BF02733547
- 471 Hesse, M., & Birn, J. (2004, February). On the cessation of magnetic reconnection.  
472 *Annales Geophysicae*, *22*, 603-612. doi: 10.5194/angeo-22-603-2004
- 473 Hesse, M., Birn, J., & Kuznetsova, M. (2001, March). Collisionless magnetic re-  
474 connection: Electron processes and transport modeling. *Journal of Geophysical*  
475 *Research (Space Physics)*, *106*, 3721-3736. doi: 10.1029/1999JA001002
- 476 Hesse, M., & Schindler, K. (2001, June). The onset of magnetic reconnec-  
477 tion in the magnetotail. *Earth, Planets, and Space*, *53*, 645-653. doi:  
478 10.1186/BF03353284
- 479 Hesse, M., Schindler, K., Birn, J., & Kuznetsova, M. (1999, May). The diffusion re-  
480 gion in collisionless magnetic reconnection. *Physics of Plasmas*, *6*, 1781-1795.  
481 doi: 10.1063/1.873436
- 482 Holland, D. L., & Chen, J. (1993, September). Self-consistent current sheet struc-  
483 tures in the quiet-time magnetotail. *Geophysics Research Letters*, *20*, 1775-  
484 1778. doi: 10.1029/93GL01976
- 485 Hoshino, M., Nishida, A., Mukai, T., Saito, Y., Yamamoto, T., & Kokubun, S.  
486 (1996, November). Structure of plasma sheet in magnetotail: Double-peaked  
487 electric current sheet. *Journal of Geophysical Research (Space Physics)*, *101*,  
488 24775-24786. doi: 10.1029/96JA02313

- 489 Ipavich, F. M., Galvin, A. B., Gloeckler, G., Hovestadt, D., Klecker, B., & Sc-  
 490 holer, M. (1984, May). Energetic (greater than 100 keV) O(+) ions  
 491 in the plasma sheet. *Geophysics Research Letters*, *11*, 504-507. doi:  
 492 10.1029/GL011i005p00504
- 493 Israelevich, P. L., & Ershkovich, A. I. (2006, July). Bifurcation of Jovian magneto-  
 494 tail current sheet. *Annales Geophysicae*, *24*, 1479-1481. doi: 10.5194/angeo-24  
 495 -1479-2006
- 496 Israelevich, P. L., & Ershkovich, A. I. (2008, June). Bifurcation of the tail current  
 497 sheet and ion temperature anisotropy. *Annales Geophysicae*, *26*, 1759-1765.  
 498 doi: 10.5194/angeo-26-1759-2008
- 499 Karimabadi, H., Daughton, W., & Quest, K. B. (2005, March). Antiparallel versus  
 500 component merging at the magnetopause: Current bifurcation and intermit-  
 501 tent reconnection. *Journal of Geophysical Research (Space Physics)*, *110*,  
 502 A03213. doi: 10.1029/2004JA010750
- 503 Karimabadi, H., Pritchett, P. L., Daughton, W., & Krauss-Varban, D. (2003,  
 504 November). Ion-ion kink instability in the magnetotail: 2. Three-dimensional  
 505 full particle and hybrid simulations and comparison with observations. *Jour-  
 506 nal of Geophysical Research (Space Physics)*, *108*, 1401. doi: 10.1029/  
 507 2003JA010109
- 508 Karimabadi, H., Roytershteyn, V., Mouikis, C. G., Kistler, L. M., & Daughton,  
 509 W. (2011, May). Flushing effect in reconnection: Effects of minority  
 510 species of oxygen ions. *Planetary and Space Science*, *59*, 526-536. doi:  
 511 10.1016/j.pss.2010.07.014
- 512 Kistler, L. M., Mouikis, C., Möbius, E., Klecker, B., Sauvaud, J. A., RéMe, H., ...  
 513 Balogh, A. (2005, June). Contribution of nonadiabatic ions to the cross-  
 514 tail current in an O<sup>+</sup> dominated thin current sheet. *Journal of Geophysical  
 515 Research (Space Physics)*, *110*, A06213. doi: 10.1029/2004JA010653
- 516 Kronberg, E. A., Ashour-Abdalla, M., Dandouras, I., Delcourt, D. C., Grigorenko,  
 517 E. E., Kistler, L. M., ... Zelenyi, L. M. (2014, November). Circulation  
 518 of Heavy Ions and Their Dynamical Effects in the Magnetosphere: Re-  
 519 cent Observations and Models. *Space Science Review*, *184*, 173-235. doi:  
 520 10.1007/s11214-014-0104-0
- 521 Lottermoser, R.-F., Scholer, M., & Matthews, A. P. (1998, March). Ion kinetic ef-

- 522           fects in magnetic reconnection: Hybrid simulations. *Journal of Geophysical Re-*  
523           *search (Space Physics)*, *103*, 4547-4560. doi: 10.1029/97JA01872
- 524   Lyons, L. R., & Speiser, T. W. (1982, April). Evidence for current sheet acceleration  
525           in the geomagnetic tail. *Journal of Geophysical Research*, *87*, 2276-2286. doi:  
526           10.1029/JA087iA04p02276
- 527   Markidis, S., Lapenta, G., Bettarini, L., Goldman, M., Newman, D., & Andersson,  
528           L. (2011, September). Kinetic simulations of magnetic reconnection in pres-  
529           ence of a background O<sup>+</sup> population. *Journal of Geophysical Research (Space*  
530           *Physics)*, *116*, A00K16. doi: 10.1029/2011JA016429
- 531   Meng, C.-I., Lui, A. T. Y., Krimigis, S. M., Ismail, S., & Williams, D. J. (1981,  
532           July). Spatial distribution of energetic particles in the distant magne-  
533           totail. *Journal of Geophysical Research*, *86*, 5682-5700. doi: 10.1029/  
534           JA086iA07p05682
- 535   Nakamura, R., Baumjohann, W., Runov, A., Volwerk, M., Zhang, T. L., Klecker, B.,  
536           ... Frey, H. U. (2002, December). Fast flow during current sheet thinning.  
537           *Geophysics Research Letters*, *29*, 2140. doi: 10.1029/2002GL016200
- 538   Ricci, P., Lapenta, G., & Brackbill, J. U. (2002, December). GEM reconnection  
539           challenge: Implicit kinetic simulations with the physical mass ratio. *Geophysics*  
540           *Research Letters*, *29*, 2088. doi: 10.1029/2002GL015314
- 541   Ricci, P., Lapenta, G., & Brackbill, J. U. (2004, March). Structure of the magne-  
542           totail current: Kinetic simulation and comparison with satellite observations.  
543           *Geophysics Research Letters*, *31*, L06801. doi: 10.1029/2003GL019207
- 544   Runov, A., Nakamura, R., Baumjohann, W., Treumann, R. A., Zhang, T. L., Volw-  
545           erk, M., ... Kistler, L. (2003, June). Current sheet structure near magnetic  
546           X-line observed by Cluster. *Geophysics Research Letters*, *30*, 1579. doi:  
547           10.1029/2002GL016730
- 548   Runov, A., Nakamura, R., Baumjohann, W., Zhang, T. L., Volwerk, M., Eichel-  
549           berger, H.-U., & Balogh, A. (2003, January). Cluster observation of a  
550           bifurcated current sheet. *Geophysics Research Letters*, *30*, 1036. doi:  
551           10.1029/2002GL016136
- 552   Runov, A., Sergeev, V., Nakamura, R., Baumjohann, W., Vörös, Z., Volwerk,  
553           M., ... Balogh, A. (2004, July). Properties of a bifurcated current sheet  
554           observed on 29 August 2001. *Annales Geophysicae*, *22*, 2535-2540. doi:

- 555 10.5194/angeo-22-2535-2004
- 556 Runov, A., Sergeev, V. A., Nakamura, R., Baumjohann, W., Apatenkov, S., Asano,  
557 Y., ... Balogh, A. (2006, March). Local structure of the magnetotail current  
558 sheet: 2001 Cluster observations. *Annales Geophysicae*, *24*, 247-262. doi:  
559 10.5194/angeo-24-247-2006
- 560 Sergeev, V., Runov, A., Baumjohann, W., Nakamura, R., Zhang, T. L., Volwerk,  
561 M., ... Klecker, B. (2003, March). Current sheet flapping motion and  
562 structure observed by Cluster. *Geophysics Research Letters*, *30*, 1327. doi:  
563 10.1029/2002GL016500
- 564 Sergeev, V. A., Mitchell, D. G., Russell, C. T., & Williams, D. J. (1993, October).  
565 Structure of the tail plasma/current sheet at  $\sim 11 R_E$  and its changes in the  
566 course of a substorm. *Journal of Geophysical Research*, *98*, 17345-17366. doi:  
567 10.1029/93JA01151
- 568 Shay, M. A., Drake, J. F., & Swisdak, M. (2007, October). Two-Scale Struc-  
569 ture of the Electron Dissipation Region during Collisionless Magnetic Re-  
570 connection. *Physical Review Letters*, *99*(15), 155002. doi: 10.1103/  
571 PhysRevLett.99.155002
- 572 Shelley, E. G., Johnson, R. G., & Sharp, R. D. (1972). Satellite observations of ener-  
573 getic heavy ions during a geomagnetic storm. *Journal of Geophysical Research*,  
574 *77*, 6104. doi: 10.1029/JA077i031p06104
- 575 Sitnov, M. I., Guzdar, P. N., & Swisdak, M. (2003, July). A model of the bifur-  
576 cated current sheet. *Geophysics Research Letters*, *30*, 1712. doi: 10.1029/  
577 2003GL017218
- 578 Sitnov, M. I., Swisdak, M., Guzdar, P. N., & Runov, A. (2006, August). Structure  
579 and dynamics of a new class of thin current sheets. *Journal of Geophysical Re-*  
580 *search (Space Physics)*, *111*, A08204. doi: 10.1029/2005JA011517
- 581 Speiser, T. W. (1965, September). Particle Trajectories in Model Current Sheets, 1,  
582 Analytical Solutions. *Journal of Geophysical Research*, *70*, 4219-4226. doi: 10  
583 .1029/JZ070i017p04219
- 584 Thompson, S. M., Kivelson, M. G., El-Alaoui, M., Balogh, A., RéMe, H., & Kistler,  
585 L. M. (2006, March). Bifurcated current sheets: Statistics from Cluster magne-  
586 tometer measurements. *Journal of Geophysical Research (Space Physics)*, *111*,  
587 A03212. doi: 10.1029/2005JA011009

- 588 Villasenor, J., & Buneman, O. (1992, March). Rigorous charge conservation for local  
589 electromagnetic field solvers. *Computer Physics Communications*, *69*, 306-316.  
590 doi: 10.1016/0010-4655(92)90169-Y
- 591 Wygant, J. R., Cattell, C. A., Lysak, R., Song, Y., Dombeck, J., McFadden, J., ...  
592 Mouikis, C. (2005, September). Cluster observations of an intense normal  
593 component of the electric field at a thin reconnecting current sheet in the tail  
594 and its role in the shock-like acceleration of the ion fluid into the separatrix  
595 region. *Journal of Geophysical Research (Space Physics)*, *110*, A09206. doi:  
596 10.1029/2004JA010708
- 597 Zelenyĭ, L. M., Malova, H. V., & Popov, V. Y. (2003, September). Splitting of Thin  
598 Current Sheets in the Earth's Magnetosphere. *Soviet Journal of Experimental  
599 and Theoretical Physics Letters*, *78*, 296-299. doi: 10.1134/1.1625728

**Figure.**

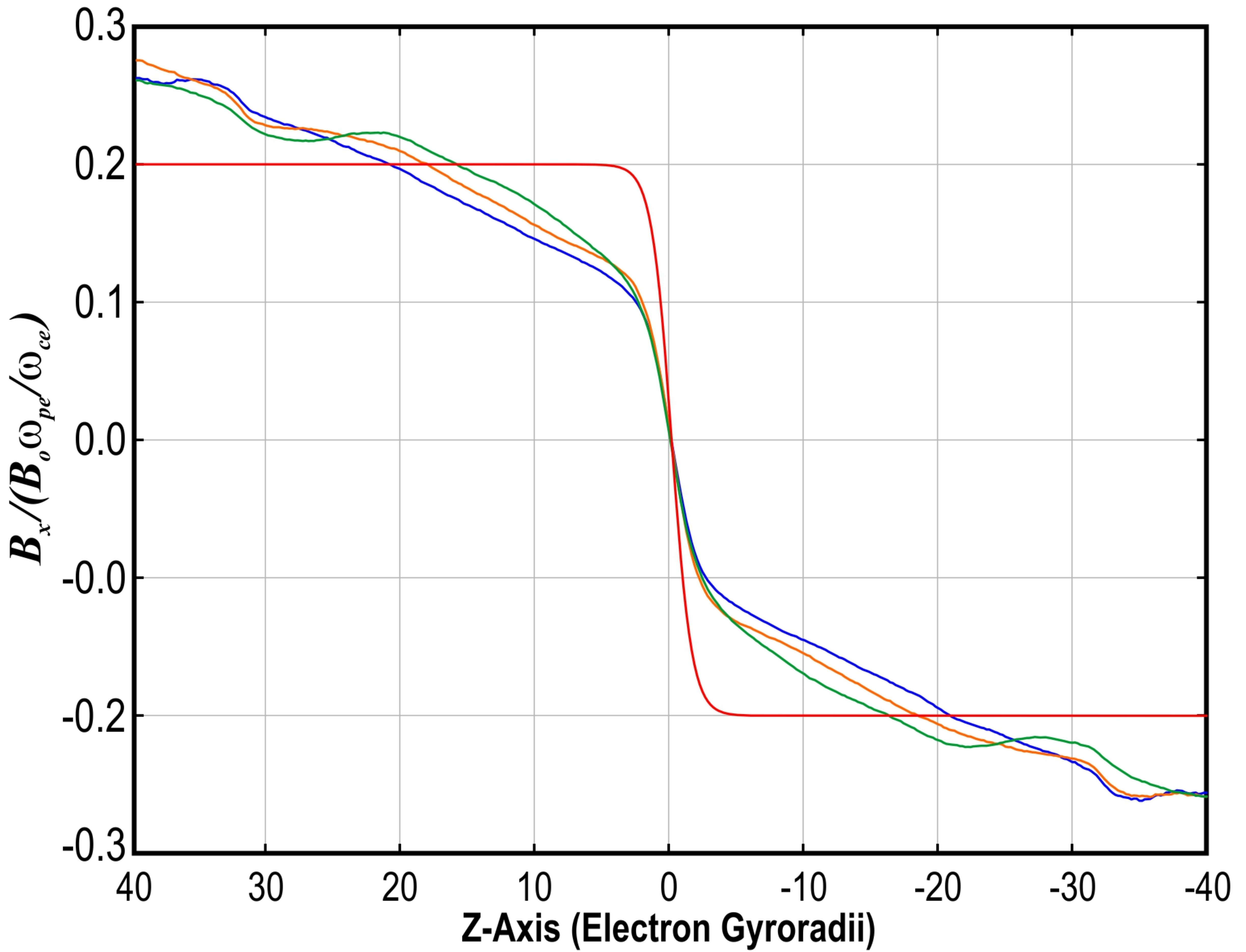


**Figure.**

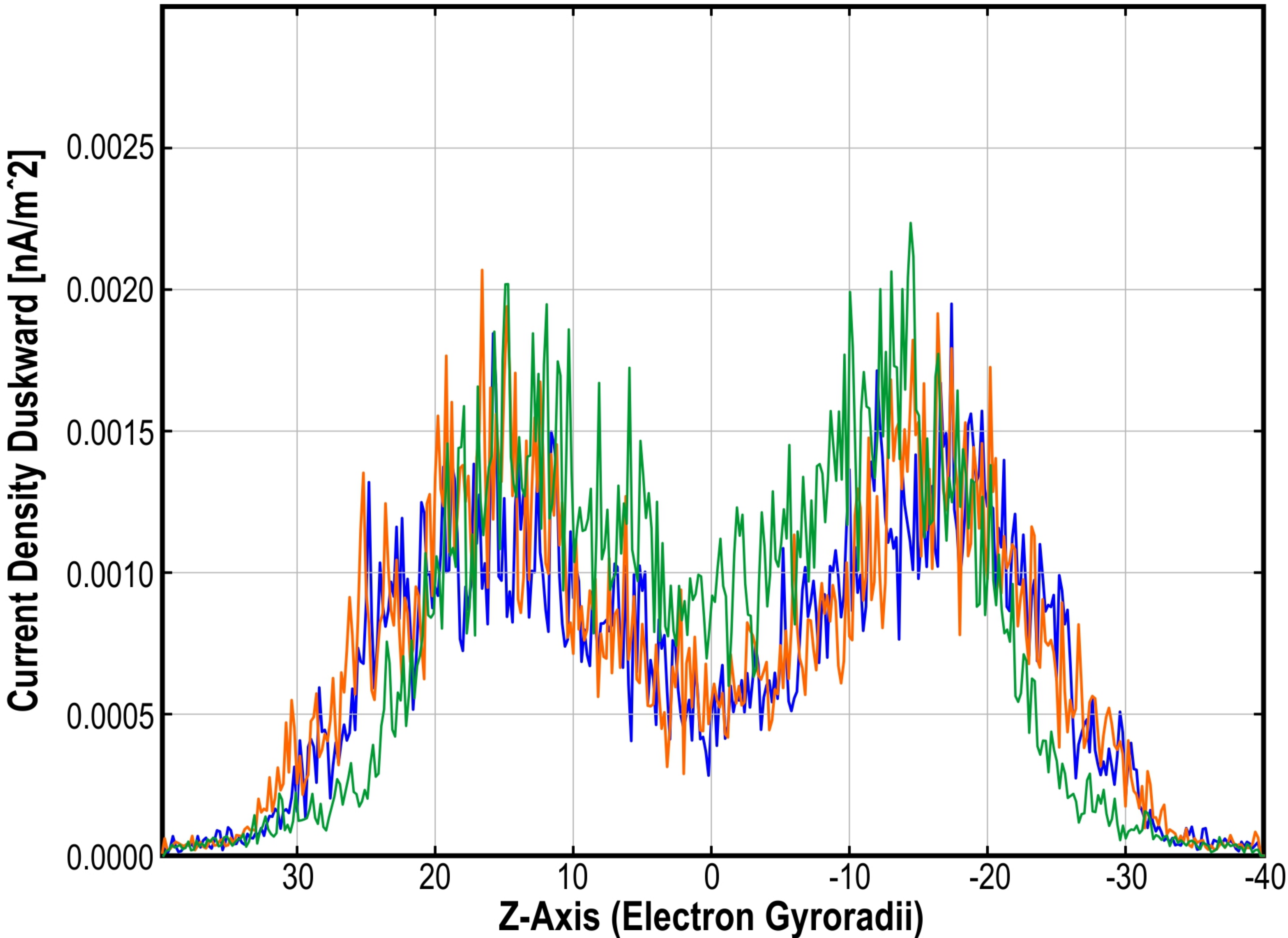


**Figure.**

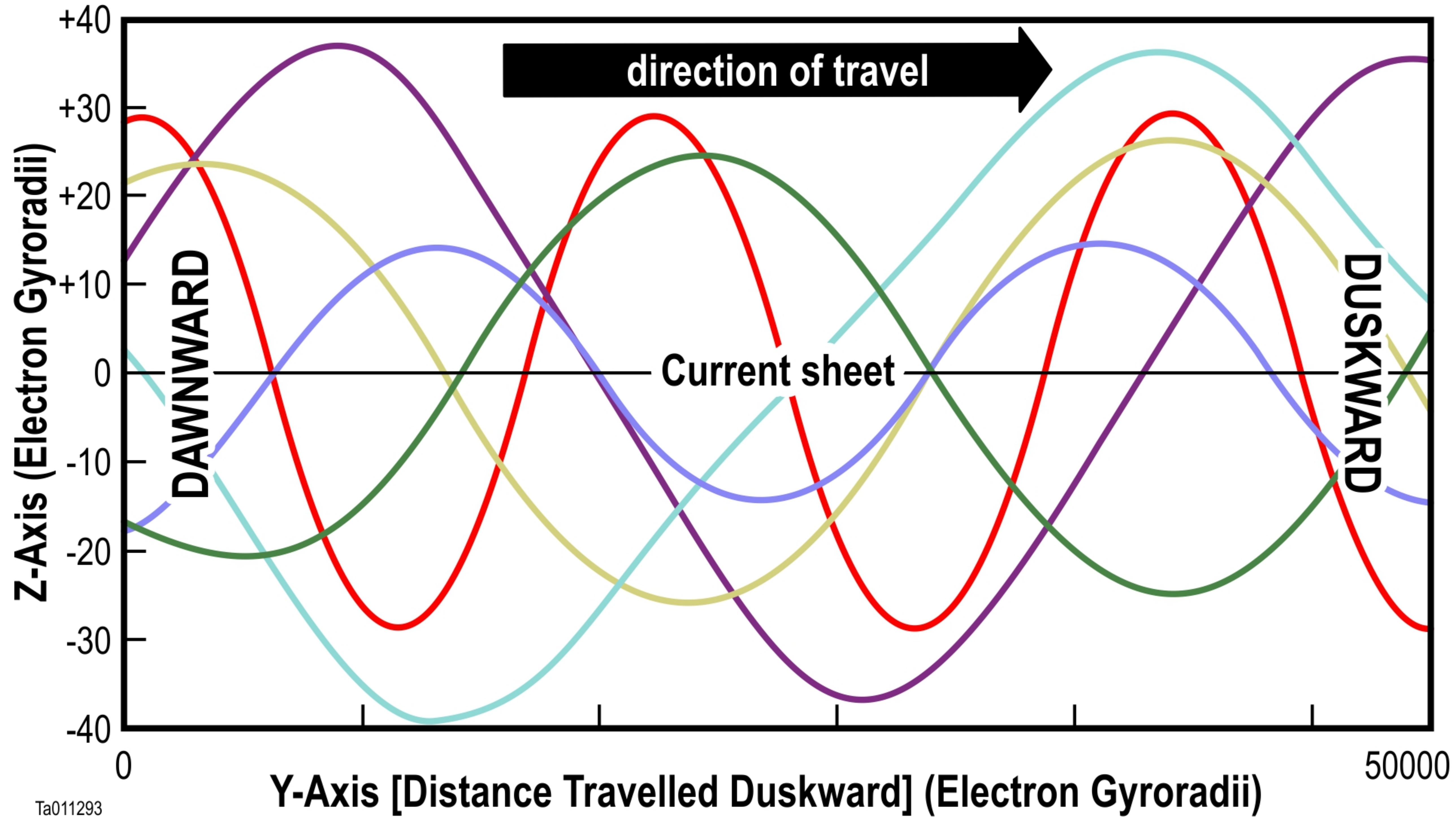
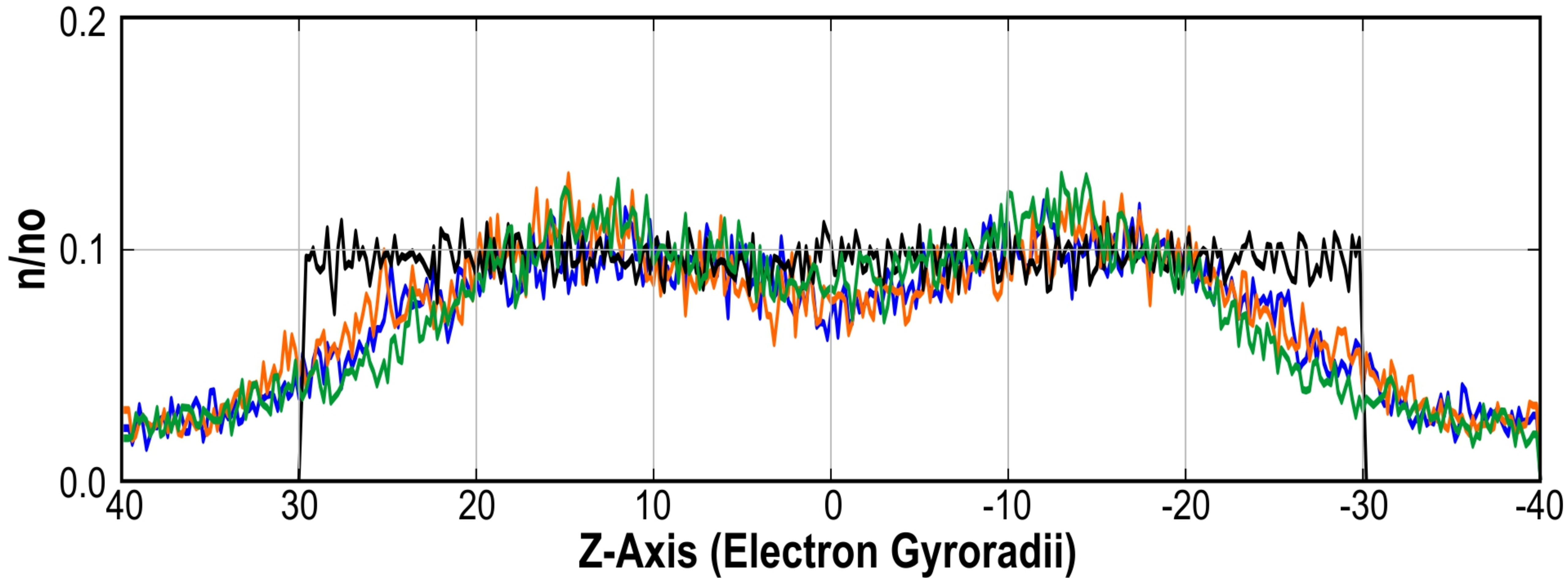


Figure.



**Figure.**

